Research Article | Vol. 30, No. 25 / 5 Dec 2022 / Optics Express 44983
Optics EXPRESS

Anomalous π modes by Floquet engineering in optical lattices with long-range coupling

SHENGJIE WU,[1] WANGE SONG,[1,2] ZHIYUAN LIN,[1] CHEN CHEN,[1] SHINING ZHU,[1] AND TAO LI[1,3]

[1]National Laboratory of Solid State Microstructures, Key Laboratory of Intelligent Optical Sensing and Manipulations, Jiangsu Key Laboratory of Artificial Functional Materials, College of Engineering and Applied Sciences, Nanjing University, Nanjing, 210093, China
[2]songwange@nju.edu.cn
[3]taoli@nju.edu.cn

Abstract: Photonic Floquet topological insulators provide a powerful tool to manipulate the optical fields, which have been extensively studied with only nearest-neighbor coupling. Here, we demonstrate that nontrivial Floquet topological phase and photonic π modes are brought from long-range coupling in a one-dimensional periodically driven optical lattice. Interestingly, the long-range coupling is found to give rise to new Floquet π modes that do not exist in the traditional Floquet lattices. We interpret the underlying physics by analyzing the replica bands, which shows quasienergies band crossing and reopening of new nontrivial π gaps due to the long-range coupling. Our results provide a new route in manipulating optical topological modes by Floquet engineering with long-range coupling.

1. Introduction

Topological photonics has attracted considerable interest due to the fascinating photonic topological states, which give rise to plenty of novel functionalities with robust properties [1–3]. Recently, periodical modulation has been utilized as a powerful tool to manipulate optical field, which leads to novel light behaviors inaccessible in static systems, such as dynamic localization [4], dispersionless coupling [5], and photonic Floquet topological insulators [6]. In particular, the periodical modulation on a typical one-dimensional (1D) Su-Schrieffer-Heeger (SSH) model has demonstrated new topological modes, known as the π modes [7–10], which exhibit oscillation behavior on the edge of lattice and are quite different from the celebrate zero modes in the static SSH model [11,12]. To be mentioned, in most previous studies, only the nearest-neighbor couplings are considered, while the long-range couplings from nonadjacent lattices are neglected or make little contribution [13]. In fact, the long-range coupling can lead to new effects [14–27], while remains largely unexplored in Floquet optical systems. Recently, new topological phases by long-range coupling have been revealed with fast Floquet modulation (i.e., in the high-frequency limit) [14,19]. However, the subtle interactions between Floquet bands are neglected, which play a key role in generating the π modes.

In this paper, we show that long-range coupling can induce new Floquet topological phases (FTP) and anomalous π modes in periodically driven SSH waveguide lattice. By incorporating the long-range coupling, we construct a topological phase diagram to illustrate the new FTP transitions. It is found that the long-range coupling can turn a topologically trivial Floquet lattice to a nontrivial one by opening the π gap and ensures the emergence of the π mode. We give a clear interpretation of the emergence of the new Floquet modes by analyzing the interacting replica bands, which are further verified by the calculation of topological invariant G_π. Our work demonstrates new features of long-range coupling for nontrivial optical state manipulations and suggests more explorations in Floquet optical lattice.

#476899 https://doi.org/10.1364/OE.476899
Journal © 2022 Received 30 Sep 2022; revised 1 Nov 2022; accepted 2 Nov 2022; published 23 Nov 2022

Optics EXPRESS

2. Results and discussions

2.1. Model

We start with considering a 1D optical lattice containing A and B sites (e.g., binary waveguide array), as the schematics of the cross-section shown in Fig. 1(a). The Hamiltonian of this lattice with the first and the third NN couplings can be expressed as follows (the second NN couplings would break the chiral symmetry and not be considered here [25]):

$$H(z) = \sum_j \begin{pmatrix} c_{11}(z)a^{\dagger}_{B,j}a_{A,j} + c_{12}(z)a^{\dagger}_{A,j+1}a_{B,j} \\ +c_{31}(z)a^{\dagger}_{B,j+1}a_{A,j} + c_{32}(z)a^{\dagger}_{A,j+2}a_{B,j} \end{pmatrix} + h.c., \tag{1}$$

where $a_{A,j}$ and $a_{B,j}$ donate the annihilation operators in sub-lattices A and B in the jth unit cell, respectively. Both the first and the third NN couplings $c_{11(2)}$ and $c_{31(2)}$ are periodically modulated along the propagation distance z, i.e., $c_{11} = c_{10}\text{-}\delta c_1\cos(\omega z+\varphi)$, $c_{12} = c_{10}+\delta c_1\cos(\omega z+\varphi)$, $c_{31} = c_{30}\text{-}\delta c_3\cos(\omega z+\varphi)$, $c_{32} = c_{30}+\delta c_3\cos(\omega z+\varphi)$, where c_{10} and c_{30} are the couplings without bending, δc_1 and δc_3 denote the amplitudes of modulation and ω ($\omega \equiv 2\pi/P$, P is the period) is the modulation frequency. φ is the initial phase determined by the starting distance $z = 0$, i.e., Floquet gauge [7], which is set to zero without loss of generality. With periodic boundary condition (PBC), the Hamiltonian can be transformed into momentum space:

$$\begin{aligned} H(k,z) &= [c_{11}(z) + c_{12}(z)\cos(k) + c_{31}(z)\cos(k) + c_{32}(z)\cos(2k)]\sigma_x \\ &+[c_{12}(z)\sin(k) - c_{31}(z)\sin(k) + c_{32}(z)\sin(2k)]\sigma_y, \end{aligned} \tag{2}$$

where k is the quasi-momentum, and $\sigma_{x(y)}$ is the Pauli operator. Note that this Hamiltonian possesses a chiral symmetry defined by σ_z due to the anticommutation relation $\{H(k, z), \sigma_z\} = 0$ [8].

To clearly show the influence of long-range coupling on the band structure, we first consider the static case, i.e., $\delta c_1 = \delta c_3 \equiv 0$, and Eq. (2) writes

$$\begin{aligned} H_0 &= [c_{10} + c_{10}\cos(k) + c_{30}\cos(k) + c_{30}\cos(2k)]\sigma_x \\ &+[c_{10}\sin(k) - c_{30}\sin(k) + c_{30}\sin(2k)]\sigma_y. \end{aligned} \tag{3}$$

Figures 1(b)–1(e) shows the corresponding band structure with $c_{30}/c_{10} = 0$, 0.5, 1, and ∞, respectively. The long-range coupling leads to two major consequences: (1) much broader bandwidth $\Delta\varepsilon_{\max}$, i.e., the bandwidth increases with the strength of long-range coupling [Figs. 1(d) and 1(f)]; (2) the emergence of another pair of degenerate points (DPs) for $c_{30}/c_{10} > 1/3$ [Figs. 1(d) and 1(g)], which indicates richer topological phases (see Supplement 1 for more discussions).

2.2. Long-rang coupling induced π modes

Then we consider the periodically driven case with nonzero δc_1 and δc_3. Note that we set $c_{32}(z) \equiv 0$ in the following calculation to simplify the model while preserving the basic effects [$c_{31} = c_{30}\text{-}\delta c_3\cos(\omega z)$]. Besides, a possible realization of the model with $c_{32}(z) \equiv 0$ is proposed in a ladder waveguide system (see Supplement 1). According to the Floquet theory, the evolution of our lattice with Hamiltonian $H(z)$ (Eq. (1)) is governed by the evolution operator [8]:

$$U(z) = \hat{T}e^{-i\int_0^z H(z')dz'}, \tag{4}$$

where $\hat{T}$ denotes the time-ordering operator. The Floquet operator corresponds to the evolution operator for one full period P, given by $U(P)$, from which a z-averaged effective Hamiltonian can

Optics EXPRESS

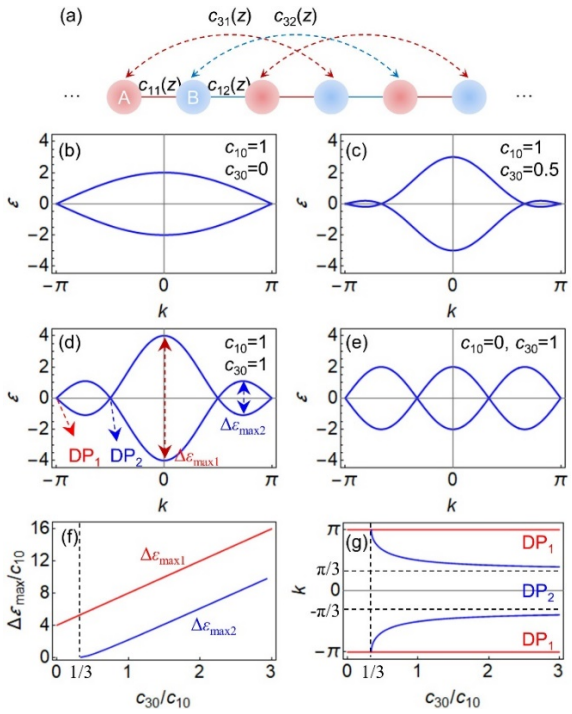

Fig. 1. (a) Schematics of the one-dimensional lattice with the NN coupling c11(2) and 3rd NN coupling c31(2). (b-e) Band structure in the static case under periodic boundary condition (PBC) with c30/c10 = 0, 0.5, 1, and ∞, respectively. (f) The bandwidth Δεmax1 and Δεmax2 as a function of c30/c10. (g) The positions of two pairs of DPs (DP1 and DP2) in the momentum space as a function of c30/c10.

be defined as

$$H_{eff} = (i/P)\ln U(P). \tag{5}$$

The eigenvalues of H_{eff} correspond to the quasienergies spectrum of the lattice, in analogy to the eigenenergies in a static one. We first calculate the quasienergies (ε) band structure under open boundary conditions (OBCs) with 80 sites as a function of $\omega/4c_{10}$ with only nearest-neighbor coupling (with $c_{10} = 1$, $\delta c_1 = 0.5$, $c_{30} = 0$, $\delta c_3 = 0$) [Fig. 2(a)]. It is clearly observed that a π mode (highlighted in red, ε=-π is equivalent to ε=π) emerges in the frequency region of ($4c_{10}/3$, $4c_{10}$) [28–30]. As an example, Fig. 2(c) shows the z-dependent evolution of the π edge modes with ω=$2c_{10}$, which propagate along the boundaries and exhibit periodic oscillation in the intensity distribution. However, as we gradually increase the driven frequency to the higher-frequency regime ω>$4c_{10}$, the fast modulation would smear out the z-periodic staggered coupling and renders the lattice similar to the static case with identical couplings, which belongs to the trivial phase without π modes [Fig. 2(d) with $\omega/4c_{10} = 1.5$].

Interestingly, with the presence of long-range coupling (e.g., the third NN coupling), it is possible to retrieve the π modes. Figure 2(b) shows the quasienergy band structure as a function of c_{30}/c_{10} with $c_{10} = 1$, $\delta c_1 = 0.5$, $\delta c_3 = 0.5c_{30}$, $\omega/4c_{10} = 1.5$ (no π mode with only NN coupling). It is found that a discrete mode gradually stands out from bulk modes as c_{30}/c_{10} increases close to 1 and turns into a π mode for $1 < c_{30}/c_{10} < 3$ [see the zoom-in figure in right panel of Fig. 2(b)]. The z-dependent evolution of the π mode at $c_{30}/c_{10} = 2$ is, as for example shown in Fig. 2(e), which exhibits similar periodic oscillation features as the original π mode [Fig. 2(c)]. This is the π edge mode retrieved by the long-range coupling. Intriguingly, one finds that when c_{30}/c_{10}

Optics EXPRESS

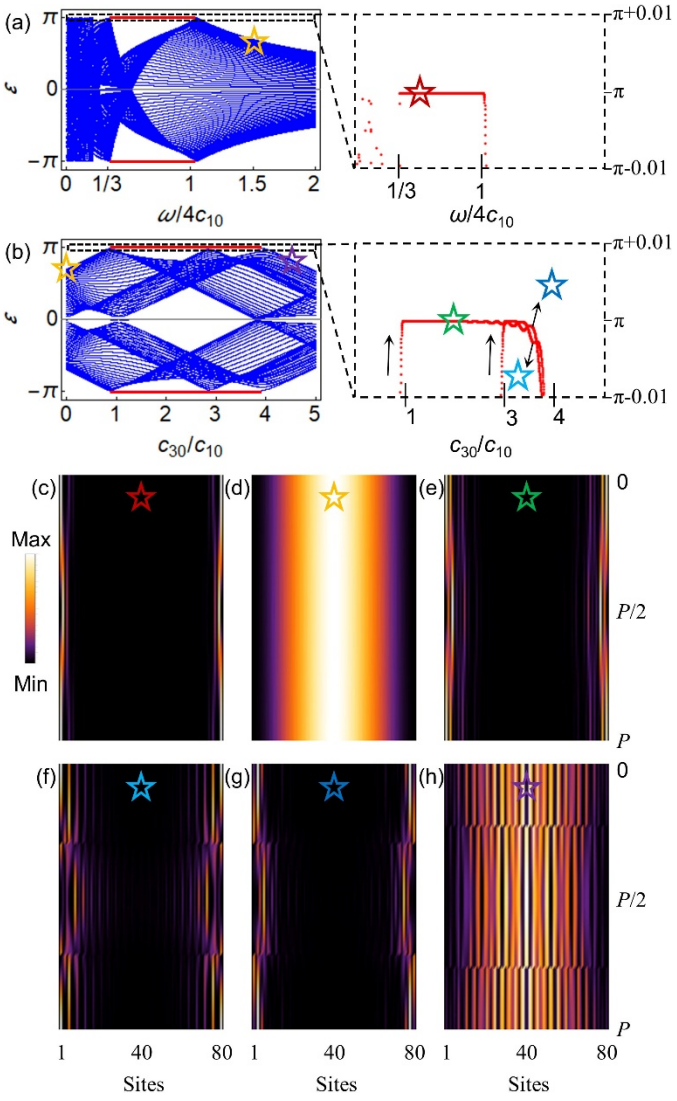

Fig. 2. (a) Quasienergies spectrum under open boundary condition (OBC) with 80 sites as a function of ω without long-range coupling, i.e., $c_{30} = 0$. (b) Quasienergies spectrum as a function of c_{30} with $\omega/4c_{10}$ fixed at 1.5. The π modes are highlighted by red lines. Right panels: zoom-in spectrum of the π modes. The red, orange, green, light blue, dark blue, and purple pentagrams mark the quasi-eigenmodes shown in (c)-(h). (c)-(h) The dynamic evolutions of the π edge states and trivial extended states corresponding to cases marked by pentagrams with different colors in (a) and (b).

Optics EXPRESS

further increases crossing 3, another bulk mode also gradually turns into the π mode, while the former π mode remains. Thus, there are two π modes in the range of $3 < c_{30}/c_{10} < 4$ [see the zoom-in figure in right panel of Fig. 2(b) and the field distributions are shown in Figs. 2(f) and (g) with $c_{30}/c_{10} = 3.5$]. Similar to the original π mode, the new π mode mainly locates on the edge of the lattice and periodically oscillates with the same period as the Floquet modulation. The field distribution of the new π mode penetrates more into the bulk than the original one, which is caused by the stronger long-range couplings. As we continue to increase the long-range coupling to exceed $c_{30}/c_{10} = 4$, all π modes vanish and only bulk states are left [see Fig. 2(h) with $c_{30}/c_{10} = 4.5$].

2.3. Floquet replica band analysis

To understand the emergence and elimination of π modes by long-range coupling, we adopt the extended Hilbert space R⊗P, which is a direct product of the usual Hilbert space R and the space P of z-periodic functions spanned by $e^{i(n\omega z)}$, where the index n defines a subspace called Floquet replica (see Supplement 1) [8,9]. The underlying physics becomes much clearer by analyzing the replica bands. Figure 3 shows the calculated replica bands for different c_{30}/c_{10} with $\omega/4c_{10} = 1.5$ under PBCs. The zoom-in band structures around $\varepsilon = \omega/2$ are also shown in the insets.

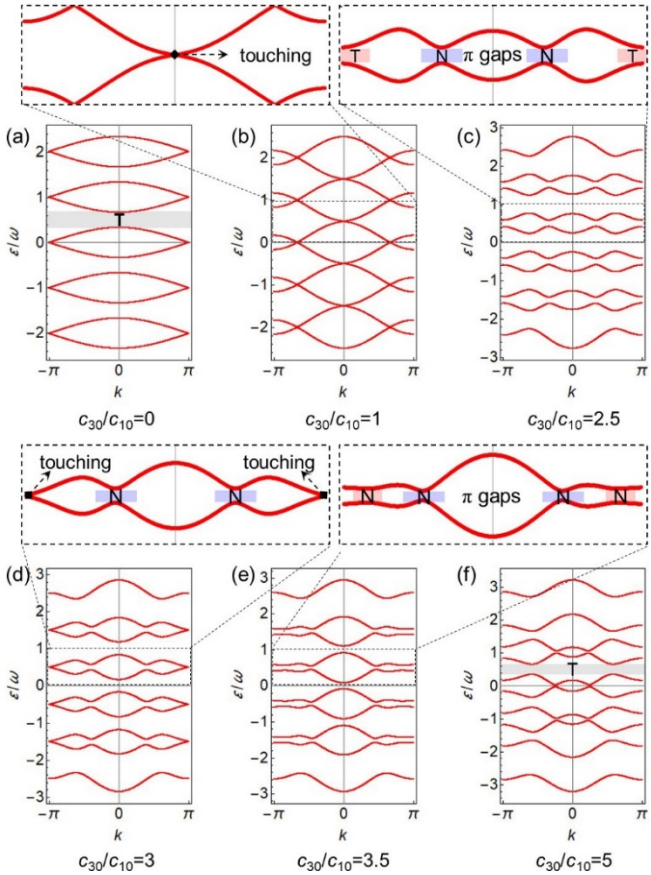

Fig. 3. (d) The momentum space quasienergy band structures of the five chosen frequency replicas with $c_{30}/c_{10} = 0$, 1, 2.5, 3, 3.5, and 5. The inserts show the enlarged band of replica coupling between $n = 0$ and 1, where the band touching and trivial (T)/nontrivial (N) π gaps are marked.

Optics EXPRESS

For $c_{30}/c_{10}= 0$ as the traditional case, each replica is decoupled from others with a trivial (T) gap. However, when long-range coupling is introduced, the bandwidth of each replica expands [as have been shown in Fig. 1(f)], and the gap just closes due to the band touching of the expanded replicas at $k = 0$ with $c_{30}/c_{10} = 1$ [see enlarged picture in Fig. 3(b)]. With further increasing c_{30}/c_{10}, the coupling between replicas opens this gap again, as shown in Fig. 3(c) with $c_{30}/c_{10} = 2.5$. This gap closing-reopening process switches the π gap from trivial to nontrivial (N) and implies the emergence of π modes for a finite lattice. Intriguingly, further increasing c_{30}/c_{10} would enable another band touching at $k=\pm\pi$ [$c_{30}/c_{10} = 3$, see Fig. 3(d) and the enlarged picture] and switch another π gap from trivial to nontrivial [$c_{30}/c_{10} = 3.5$, see Fig. 3(e) and the enlarged picture]. Thus, more π modes can be expected. However, when $c_{30}/c_{10} > 4$, more Floquet replicas are involved and the π gaps become trivial [Fig. 3(f) with $c_{30}/c_{10} = 5$], thus all π modes are eliminated. The replica analysis clearly demonstrates the underlying physics of the emergence and elimination of π modes by long-range coupling shown in Fig. 2.

2.4. Topological invariant and phase diagram

We further verify our findings through the calculation of the topological invariant. For the 1D Floquet SSH model with long-range coupling, the chiral symmetry preserves and a $\mathbb{Z}$-valued invariant G_π characterizing the topological feature of quasienergy gap at $\varepsilon=\pi$ can be defined [30]. The invariant G_π is generated from the periodized evolution operator $V(z, k)$, which is defined as:

$$V(z,k) \equiv U(z,k)e^{iH_{eff}(k)z}, \tag{6}$$

where $U(z,k)$ is the evolution operator and $H_{\text{eff}}(k)$ is the z-averaged Hamiltonian. G_π characterize the winding number of $V_\pi{}^+$ around the origin in the k-space [8,9,30]:

$$G_\pi = \deg(V_\pi^+) = \frac{i}{2\pi}\int_{-\pi}^{\pi} tr[(V_\pi^+)^{-1}\partial_k V_\pi^+]dk, \tag{7}$$

where $V_\pi{}^+$ is the diagonal element of $V(z, k)$ at half period:

$$V(\frac{P}{2},k) = \begin{pmatrix} V_\pi^+ & 0 \\ 0 & V_\pi^- \end{pmatrix}. \tag{8}$$

Here, the calculated G_π with varying c_{30}/c_{10} and $\omega/4c_{10}$ are shown in Fig. 4 (upper panel). It is observed that both the driven frequency and long-range coupling can modulate the Floquet topological phases (FTP) of the lattice. Region I (white region) represents trivial phase ($G_\pi = 0$) without the π mode, while nontrivial π gap opens and π modes emerge in regions II ($G_\pi = 1$, blue region) and III ($G_\pi = 2$, red region). The boundaries between different topological phases are indicated by green lines. The FTPs with the presence of the long-range coupling are much richer compared with the traditional case (highlighted by the orange line). Notably, the long-range coupling can induce new FTP with G_π greater than one (III, red region), which has no counterpart in the traditional Floquet lattice with only NN coupling. Specifically, for $\omega/4c_{10} = 1.5$ as the case shown in Figs. 2 and 3, the dependence of G_π on long-range coupling strength c_{30}/c_{10} is shown in Fig. 4 (bottom panel). For $c_{30}/c_{10} = 0$, $G_\pi = 0$ indicates a trivial case. When increasing c_{30}/c_{10} crossing 1, G_π sharply changes to 1, indicating nontrivial FTP and the emergence of topological π mode. When c_{30}/c_{10} further increases within the range of $3 < c_{30}/c_{10} < 4$, the topological invariant G_π increases to 2 that implies more π modes according to the bulk-edge correspondence. Many more replicas are involved for $c_{30}/c_{10} > 4$ and the π gap becomes trivial and G_π decreases to zero. The calculated G_π fully confirms our replica analysis in Fig. 3 and is consistent with the number of topological π modes shown in Fig. 2(b). Moreover, it is found that FTP with $G_\pi>2$ can also be realized with nonzero $c_{32}(z)$, which promises the emergence of more π modes (see Supplement 1).

Optics EXPRESS

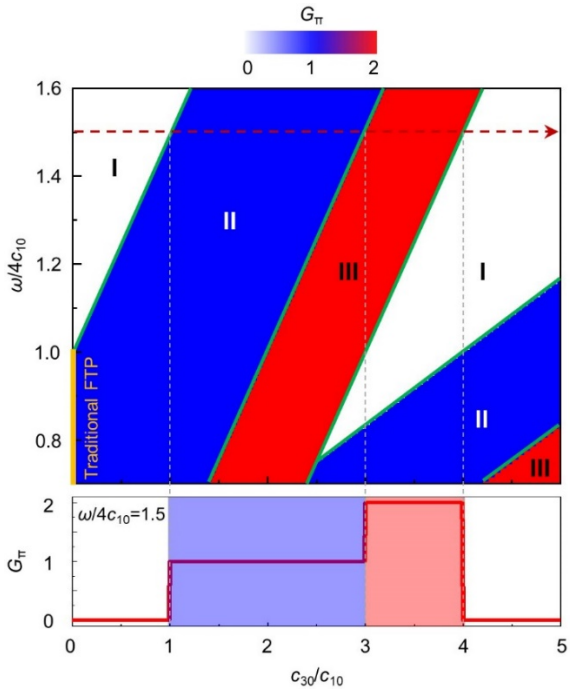

Fig. 4. Topological invariant G_π and Floquet topological phase diagram as functions of driven frequency $\omega/4c_{10}$ and long-range coupling c_{30}/c_{10}. Green lines indicate the boundary of different topological phases. The long-range coupling leads to richer FTP compared to traditional case with only NN coupling (represented by the orange line). The red dotted arrow indicates the trajectory of topological phase transition of increasing c_{30} shown in Figs. 2 and 3, corresponding to bottom panel that depicts the G_π with fixed $\omega/4c_{10} = 1.5$.

3. Conclusion

In conclusion, we have demonstrated the Floquet engineering with long-range coupling in 1D periodically driven optical lattice. The long-range coupling can open nontrivial π gaps and create unprecedented nontrivial FTP, which indicates new topological π modes. We verify our finding by the analysis of Floquet replica bands, and further calculation of topological invariant is fully consistent with this analysis. The possibility of accessing Floquet topological modes in the higher-frequency regime would inspire applications with nonadiabatic process and small lattice size. Our work demonstrates that long-range couplings could enrich the topological phases of Floquet systems, offering new opportunities for manipulating nontrivial photonic states with unique topological robustness. The periodically driven models with long-range coupling can be realized with the ladder arrangement of bending waveguide lattice based on femtosecond laser direct-writing technique [4,6,25]. Beyond this, it is possible to investigate more complex Floquet topological phases induced by the interplay of non-Hermiticity and long-range hopping if gain and loss are considered [9,11,24]. It has been revealed that the non-Hermitian gain and loss can modulate the quasienergy spectrum, thus induce topological phase transition and engineer Floquet π mode [9]. Complex topological phases may be discovered in the non-Hermitian Floquet waveguide lattice with long-range coupling due to rich band modulation mechanism. Besides, the topological feature of the Floquet lattice in the low-frequency regime with long-range coupling is also worth exploring, since there is more complex Floquet replica band interaction in the low-frequency regime that indicates richer topological phases [31].

Optics EXPRESS

Funding. National Key Research and Development Program of China (2022YFA1404300); National Natural Science Foundation of China (12174186, 12204233, 91850204).

Acknowledgments. Tao Li thanks the support from Dengfeng Project B of Nanjing University.

Disclosures. The authors declare no conflicts of interest.

Data availability. Data underlying the results presented in this paper are not publicly available at this time but may be obtained from the authors upon reasonable request.

Supplemental document. See Supplement 1 for supporting content.

References

1. Z. Wang, Y. Chong, J. D. Joannopoulos, and M. Soljačić, "Observation of unidirectional backscattering-immune topological electromagnetic states," Nature **461**(7265), 772–775 (2009).
2. G. Harari, M. A. Bandres, Y. Lumer, M. C. Rechtsman, Y. D. Chong, M. Khajavikhan, D. N. Christodoulides, and M. Segev, "Topological insulator laser: Theory," Science **359**(6381), 1230 (2018).
3. M. A. Bandres, S. Wittek, G. Harari, M. Parto, J. Ren, M. Segev, D. N. Christodoulides, and M. Khajavikhan, "Topological insulator laser: Experiments," Science **359**(6381), 1231 (2018).
4. A. Szameit, I. L. Garanovich, M. Heinrich, A. A. Sukhorukov, F. Dreisow, T. Pertsch, S. Nolte, A. Tunnermann, and Y. S. Kivshar, "Polychromatic dynamic localization in curved photonic lattices," Nat. Phys. **5**(4), 271–275 (2009).
5. W. Song, T. Li, S. Wu, C. Chen, Y. Chen, C. Huang, K. Qiu, S. Zhu, Y. Zou, and T. Li, "Dispersionless coupling among optical waveguide by artificial gauge field," Phys. Rev. Lett. **129**(5), 053901 (2022).
6. M. C. Rechtsman, J. M. Zeuner, Y. Plotnik, Y. Lumer, D. Podolsky, F. Dreisow, S. Nolte, M. Segev, and A. Szameit, "Photonic Floquet topological insulators," Nature **496**(7444), 196–200 (2013).
7. W. Song, Y. Chen, H. Li, S. Gao, S. Wu, C. Chen, S. Zhu, and T. Li, "Gauge-induced Floquet topological states in photonic waveguides," Laser Photonics Rev. **15**(8), 2000584 (2021).
8. Q. Cheng, Y. Pan, H. Wang, C. Zhang, D. Yu, A. Gover, H. Zhang, T. Li, L. Zhou, and S. Zhu, "Observation of anomalous π modes in photonic Floquet engineering," Phys. Rev. Lett. **122**(17), 173901 (2019).
9. S. Wu, W. Song, S. Gao, Y. Chen, S. Zhu, and T. Li, "Floquet π mode engineering in non-Hermitian waveguide lattices," Phys. Rev. Res. **3**(2), 023211 (2021).
10. J. Petráček and V. Kuzmiak, "Dynamics and transport properties of Floquet topological edge modes in coupled photonic waveguides," Phys. Rev. A **101**(3), 033805 (2020).
11. W. Song, W. Sun, C. Chen, Q. Song, S. Xiao, S. Zhu, and T. Li, "Breakup and recovery of topological zero modes in finite non-Hermitian optical lattices," Phys. Rev. Lett. **123**(16), 165701 (2019).
12. W. Song, W. Sun, C. Chen, Q. Song, S. Xiao, S. Zhu, and T. Li, "Robust and broadband optical coupling by topological waveguide arrays," Laser Photonics Rev. **14**(2), 1900193 (2020).
13. A. Szameit, T. Pertsch, S. Nolte, A. Tünnermann, and F. Lederer, "Long-range interaction in waveguide lattices," Phys. Rev. A **77**(4), 043804 (2008).
14. Q. Tong, J. An, J. Gong, H. Luo, and C. H. Oh, "Generating many Majorana modes via periodic driving: A superconductor model," Phys. Rev. B **87**(20), 201109 (2013).
15. G. Jotzu, M. Messer, R. Desbuquois, M. Lebrat, T. Uehlinger, D. Greif, and T. Esslinger, "Experimental realization of the topological Haldane model with ultracold fermions," Nature **515**(7526), 237–240 (2014).
16. D. Leykam, S. Mittal, M. Hafezi, and Y. Chong, "Reconfigurable topological phases in next-nearest-neighbor coupled resonator lattices," Phys. Rev. Lett. **121**(2), 023901 (2018).
17. L. Li, Z. Xu, and S. Chen, "Topological phases of generalized Su-Schrieffer-Heeger models," Phys. Rev. B **89**(8), 085111 (2014).
18. C. Li and A. E. Miroshnichenko, "Extended SSH model: non-local couplings and non-monotonous edge states," Physics **1**(1), 2–16 (2018).
19. B. Pérez-González, M. Bello, Á. Gómez-León, and G. Platero, "SSH model with long-range hoppings: topology, driving and disorder," arXiv arXiv:1802.03973 (2022).
20. O. Viyuela, L. Fu, and M. A. Martin-Delgado, "Chiral topological superconductors enhanced by long-range interactions," Phys. Rev. Lett. **120**(1), 017001 (2018).
21. W. DeGottardi, M. Thakurathi, S. Vishveshwara, and D. Sen, "Majorana fermions in superconducting wires: effects of long-range hopping, broken time-reversal symmetry, and potential landscapes," Phys. Rev. B **88**(16), 165111 (2013).
22. M. Li, D. Zhirihin, M. Gorlach, X. Ni, D. Filonov, A. Slobozhanyuk, A. Alù, and A. B. Khanikaev, "Higher-order topological states in photonic Kagome crystals with long-range interactions," Nat. Photonics **14**(2), 89–94 (2020).
23. L. Zhang, Y. Yang, Y. Ge, Y. Guan, Q. Chen, Q. Yan, F. Chen, R. Xi, Y. Li, D. Jia, S. Yuan, H. Sun, H. Chen, and B. Zhang, "Acoustic non-Hermitian skin effect from twisted winding topology," Nat. Commun. **12**(1), 6297 (2021).
24. Y. Yi and Z. Yang, "Non-Hermitian Skin modes induced by on-site dissipations and chiral tunneling effect," Phys. Rev. Lett. **125**(18), 186802 (2020).
25. Z. Jiao, S. Longhi, X. Wang, J. Gao, W. Zhou, Y. Wang, Y. Fu, L. Wang, R. Ren, L. Qiao, and X. Jin, "Experimentally detecting quantized Zak phases without chiral symmetry in photonic lattices," Phys. Rev. Lett. **127**(14), 147401 (2021).

Optics EXPRESS

26. Q. Cheng, H. Wang, Y. Ke, T. Chen, Y. Yu, Y. S. Kivshar, C. Lee, and Y. Pan, "Asymmetric topological pumping in nonparaxial photonics," Nat. Commun. **13**(1), 249 (2022).
27. Y. Wang, C. Sheng, Y. Lu, J. Gao, Y. Chang, X. Pang, T. Yang, S. Zhu, H. Liu, and X. Jin, "Quantum simulation of particle pair creation near the event horizon," Nat. Sci. Rev. **7**(9), 1476–1484 (2020).
28. J. K. Asbóth, B. Tarasinski, and P. Delplace, "Chiral symmetry and bulk-boundary correspondence in periodically driven one-dimensional systems," Phys. Rev. B **90**(12), 125143 (2014).
29. V. Dal Lago, M. Atala, and L. E. F. Foa Torres, "Floquet topological transitions in a driven one-dimensional topological insulator," Phys. Rev. A **92**(2), 023624 (2015).
30. M. Fruchart, "Complex classes of periodically driven topological lattice systems," Phys. Rev. B **93**(11), 115429 (2016).
31. M. Rodriguez-Vegal and B. Seradjeh, "Universal Fluctuations of Floquet Topological Invariants at Low Frequencies," Phys. Rev. Lett. **121**(3), 036402 (2018).